2008 IEEE International Conference on
Robotics and Automation
Pasadena, CA, USA, May 19-23, 2008

Control of a Class of Under-Actuated Systems with Saturation Using Hierarchical Sliding Mode

Dianwei Qian, Jianqiang Yi, *Member, IEEE*, and Dongbin Zhao, *Member, IEEE*

***Abstract*—This paper presents a control scheme of a class of under-actuated systems with saturation using hierarchical sliding mode. This class with a single input and multiple outputs is made up of several subsystems. Based on this physical structure, the hierarchical structure of the sliding mode surfaces is developed as follows. The sliding surface of every subsystem is defined. Then the sliding surface of one subsystem is selected as the first layer sliding surface. The first layer sliding surface is used to construct the second layer sliding surface with the sliding surface of another subsystem. This process continues till all the subsystem sliding surfaces are included. The hierarchical sliding mode control law is deduced by using Lyapunov theorem. On account of saturation nonlinearity of the single input, asymptotic stability of the control system is proven by nonlinear small gain theorem. Parameter ranges of the subsystem sliding surfaces are also given. In practice, simulation and experimental results show the validity of this control method.**

I. Introduction

THERE has been an increasing amount of attention to control problems of under-actuated systems in recent years [1]. Under-actuated systems with less control inputs than degrees-of-freedom are rich in extensive applications. In this paper, we focus on a class of under-actuated systems. This class with a control input and multiple outputs is rather large, including inverted pendulum systems, Pendubot, Acrobot, TORA, overhead crane, etc. These systems are often used for researches in various control methods and for education in various concepts [2]. Numerous control methods have been presented [2]–[6]. In fact, a normal state space expression can depict them. Thus, we can consider developing a general control method for the class.

Sliding mode control (SMC) is a robust control method [7]. The SMC provides a good candidate for control design of this class. But designing a common sliding surface for the control of under-actuated systems is not appropriate [8]. As far as physical structure is concerned, the class of mechanical systems consists of several subsystems. Based on this structure, some control methods have been presented. Lin [9] proposed a hierarchical fuzzy sliding mode control scheme. But they did not consider the stability of the subsystem sliding surfaces. In [10], a decoupled fuzzy sliding mode control law was designed. But it could only be applied to 2-level control. Wang [11] developed a cascade sliding mode control approach. But some controller parameters needed to be frequently switched for guaranteeing the system stability. [8] designed a hierarchical sliding mode controller with the entire stable sliding surfaces, but the method in [8] could not be general for under-actuated systems with more subsystems than two. By considering the stability of subsystems, the parameters of the subsystem sliding surfaces in the above mentioned control methods were selected as positive constants. To our knowledge there is no solution to the problem of the upper boundaries of these parameters. Moreover, the single control input of the class was considered as an ideal one in the above papers, and the input saturation was neglected. However, the reliable operation and acceptable performance of most control systems must be assessed in light of actuator saturation. In recent years, the problem of input saturation has received a mount of attention. Especially, nonlinear small gain theorem in [12] provides a good design tool.

Under considering saturation constraint of the control input of this class of SIMO under-actuated systems, this paper develops a control method using hierarchical sliding mode. The remainder is organized as follows. Section 2 describes the presented control method. On account of input saturation, stability analysis is presented by nonlinear small gain theorem in Section 3. Simulation and experimental results in Sections 4 and 5 show the feasibility of this control method, respectively. At last, conclusions are derived in Section 6.

II. Control Design

Consider the state space expression of this class of SIMO under-actuated systems with n subsystems as

$$\begin{cases} \dot{x}_1 = x_2 \\ \dot{x}_2 = \mathrm{f}_1 + \mathrm{b}_1 u \\ \dot{x}_3 = x_4 \\ \dot{x}_4 = \mathrm{f}_2 + \mathrm{b}_2 u \\ \quad\vdots \\ \dot{x}_{2n-1} = x_{2n} \\ \dot{x}_{2n} = \mathrm{f}_n + \mathrm{b}_n u \end{cases} \tag{1}$$

Here $X = [\, x_1, x_2, \ldots, x_{2n} \,]^{\mathrm{T}}$ is the state variable vector; f_i and b_i (i=1, 2, … , n) are the nonlinear functions of the state variables; and u is the single control input.

Equation (1) can express the class with different n, f_i and b_i.

Manuscript received September 12, 2007. This work was partly supported by the NSFC Projects under Grant No. 60575047, 60475030, and 60621001; National 863 Program (No.2007AA04Z239); the Outstanding Overseas Chinese Scholars Fund of Chinese Academy of Sciences (No. 2005-1-11).

D. Qian, J. Yi, and D. Zhao are with the Laboratory of Complex Systems and Intelligence Science, Institute of Automation, Chinese Academy of Sciences, Beijing, 100080, P.R. China (E-mail: dianwei.qian@ia.ac.cn).

If n=2, (1) can represent a Pendubot, an Acrobot, a TORA, etc; if n=3, it can express a series or parallel double inverted pendulum system; if n=4, it can be considered as a series triple inverted pendulum system; etc. Physical structure of the class is that they can be treated as being made up of several subsystems. For example, a series triple inverted pendulum system consists of four subsystems: upper pendulum, middle pendulum, lower pendulum, and cart. According to this viewpoint, such a system as (1) can be divided into n subsystems. The state equation of the ith subsystem is represented by

$$\begin{cases} \dot{x}_{2i-1} = x_{2i} \\ \dot{x}_{2i} = \mathrm{f}_i + \mathrm{b}_i u \end{cases} \tag{2}$$

Define its sliding surface (a linear function) as

$$s_i = c_i x_{2i-1} + x_{2i} \tag{3}$$

Here c_i is a positive constant. Differentiating s_i with respect to time t in (3), we have

$$\dot{s}_i = c_i \dot{x}_{2i-1} + \dot{x}_{2i} \tag{4}$$

Substituting (2) into (4) gives

$$\dot{s}_i = c_i x_{2i} + \mathrm{f}_i + \mathrm{b}_i u \tag{5}$$

Let $\dot{s}_i = 0$ in (5). Then the equivalent control of the ith subsystem is gotten as

$$u_{\mathrm{eq}i} = -(c_i x_{2i} + \mathrm{f}_i)/\mathrm{b}_i \tag{6}$$

According to diverse combinations of the subsystem sliding surfaces, a variety of hierarchical sliding mode control laws can be designed [8], [11]. And other control methods can be combined with the hierarchical sliding mode method [9], [10]. In this paper, the hierarchical structure of the sliding surfaces is designed in the following manner. The sliding surface of one subsystem is chosen as the first layer sliding surface S_1. Then S_1 is used to construct the second layer sliding surface S_2 with the sliding surface of another subsystem. This process continues till all the subsystem sliding surfaces are included. Without loss of generality, the subsystem sliding surface s_1 is selected as S_1. The hierarchical structure of the sliding surfaces is shown in Fig.1.

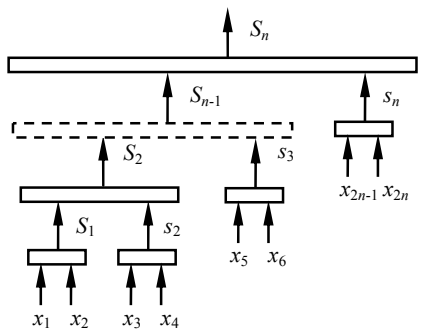

Fig. 1. Hierarchical structure of the sliding surfaces

In the presented hierarchical structure, we know that the ith layer sliding surface includes the information of the ith-subsystem sliding surface and the other i-1 lower layer sliding surfaces. As a result, the ith-layer sliding surface S_i and its control law u_i can be defined as follows.

$$S_i = \lambda_{i-1} S_{i-1} + s_i \tag{7}$$

$$u_i = u_{i-1} + u_{\mathrm{eq}i} + u_{\mathrm{sw}i} \tag{8}$$

Here $\lambda_{i\text{-}1}$ (i = 1, 2, … , n) is a constant; $\lambda_0 = S_0 = 0$; $u_0 = 0$; $u_{\mathrm{sw}i}$ (i = 1, 2, … , n) is the switching control of the ith-layer sliding surface. From the recursive formulas (7) and (8), we have

$$S_i = \sum_{r=1}^{i} (\prod_{j=r}^{i} a_j) s_r \tag{9}$$

$$u_i = \sum_{r=1}^{i} (u_{\mathrm{sw}r} + u_{\mathrm{eq}r}) \tag{10}$$

Here for a given i, $a_j = \lambda_j$ ($j \neq i$) is a constant; and $a_j = 1$ ($j = i$). The control law can be derived from Lyapunov theorem. The Lyapunov function of the ith layer is selected as

$$V_i(t) = S_i^2 / 2 \tag{11}$$

Differentiating V_i with respect to time t obtains

$$\dot{V}_i = S_i \dot{S}_i \tag{12}$$

Differentiating S_i with respect to time t in (9) and substituting it into (12) yield

$$\dot{V}_i = S_i \dot{S}_i = S_i [\sum_{r=1}^{i} (\prod_{j=r}^{i} a_j) \dot{s}_r] \tag{13}$$

Substituting (2), (4), and (10) into (13) obtains

$$\begin{aligned} \dot{V}_i &= S_i \{\sum_{r=1}^{i} [(\prod_{j=r}^{i} a_j) \cdot (c_r x_{2r} + \mathrm{f}_r + \mathrm{b}_r u_i)]\} \\ &= S_i \{\sum_{r=1}^{i} [(\prod_{j=r}^{i} a_j) \cdot \mathrm{b}_r \cdot (\sum_{\substack{l=1 \\ l \neq r}}^{i} u_{\mathrm{eq}l} + \sum_{l=1}^{i} u_{\mathrm{sw}l})]\} \\ &= S_i \cdot \{\sum_{l=1}^{i} [\sum_{\substack{r=1 \\ r \neq l}}^{i} (\prod_{j=r}^{i} a_j) \mathrm{b}_r] \cdot u_{\mathrm{eq}l} \\ &\quad + \sum_{l=1}^{i} [\sum_{r=1}^{i} (\prod_{j=r}^{i} a_j) \mathrm{b}_r] \cdot u_{\mathrm{sw}l}\} \end{aligned} \tag{14}$$

In order to have the stability of the ith-layer sliding surface, let

$$\begin{aligned} &\sum_{l=1}^{i} [\sum_{\substack{r=1 \\ r \neq l}}^{i} (\prod_{j=r}^{i} a_j) \mathrm{b}_r] \cdot u_{\mathrm{eq}l} \\ &+ \sum_{l=1}^{i} [\sum_{r=1}^{i} (\prod_{j=r}^{i} a_j) \mathrm{b}_r] \cdot u_{\mathrm{sw}l} \\ &= -k_i S_i - \eta_i \operatorname{sgn} S_i \end{aligned} \tag{15}$$

where k_i and η_i are positive constants. We have the switching control law $u_{\mathrm{sw}i}$ from (15).

$$u_{\mathrm{sw}\,i} = -\sum_{l=1}^{i-1} u_{\mathrm{sw}\,l} - \frac{\sum_{l=1}^{i}[\sum_{r=1,r\neq l}^{i}(\prod_{j=r}^{i} a_j)\,\mathrm{b}_r]u_{\mathrm{eq}\,l}}{\sum_{r=1}^{i}(\prod_{j=r}^{i} a_j)\,\mathrm{b}_r} - \frac{k_i S_i + \eta_i \operatorname{sgn} S_i}{\sum_{r=1}^{i}(\prod_{j=r}^{i} a_j)\,\mathrm{b}_r} \tag{16}$$

Substituting (16) into (10) and letting $i = n$, we can obtain the hierarchical sliding mode control law (17).

$$\begin{aligned} u_n &= \sum_{l=1}^{n-1} u_{\mathrm{sw}\,l} + u_{\mathrm{sw}\,n} + \sum_{l=1}^{n} u_{\mathrm{eq}\,l} \\ &= \frac{\sum_{r=1}^{n}(\prod_{j=r}^{n} a_j)\,\mathrm{b}_r\,u_{\mathrm{eq}\,r}}{\sum_{r=1}^{n}(\prod_{j=r}^{n} a_j)\,\mathrm{b}_r} - \frac{k_n S_n + \eta_n \operatorname{sgn} S_n}{\sum_{r=1}^{n}(\prod_{j=r}^{n} a_j)\,\mathrm{b}_r} \end{aligned} \tag{17}$$

From (17), only the switching control of the nth layer works. The switching controls of the other n-1 lower layers are merged in the deduction. In the reaching mode stage, when any state of a subsystem deviates from its own subsystem sliding surface, the switching control of the nth layer will drive it back. From the above control design, Lyapunov stability theorem can guarantee that S_i is asymptotically stable if there is no saturation constraint on the single control input. Moreover, s_i is also asymptotically stable. (If s_i is not asymptotically stable, then this contradicts the fact that S_i is asymptotically stable in (9).) However, input saturation is a common constraint and all actuators of physical devices are subject to amplitude saturation. By considering this constraint, the single control input should be written:

$$u = \mathrm{sat}(u_n) \tag{18}$$

Here sat(•) is a saturation function. sat(u_n) = u_n as | u_n| <σ and sat(u_n) = σsgn(u_n) as | u_n| ≥σ, where σ is the amplitude of the saturation function.

III. Stability Analysis

The following definitions, such as asymptotic L_∞-norm, asymptotic bound, gain function, Lipschitz well-posed system, and finite escape time, were defined in [12].

Lemma 1: Consider a Lipschitz well-posed interconnected system where the output of the hth subsystem (h=1,2) satisfies an asymptotic bound from X_h with gain γ_h and restriction Δ_h, here X_h is the state vector of the hth subsystem; γ_h is a gain function; Δ_h is a non-negative real number (or possible ∞). Suppose that for all initial conditions in X_h, there are no finite escape times. If *a)* $\Delta_2 = \infty$, *b)* $\gamma_1(\infty) \le \Delta_1$, *c)* the composition of γ_1 and γ_2 is a simple contraction, then both the outputs of the two subsystems are of asymptotic bound.

Proof: See Theorem 2 in [12]. Teel considered an interconnected system with external disturbances. But here we consider the interconnected system with no external disturbances as a special case of Teel's conclusion. Further, "subsystem" in this lemma is not a part of the under-actuated system, but a part of the interconnected system. ■

Theorem 1: Consider the SIMO under-actuated system (1) with the sliding surfaces (3), (7) and the hierarchical sliding mode control law (16). Suppose that for those initial state vectors X, there is no finite escape time. If $\sigma > |X|_a$ is satisfied, here σ is the amplitude of the saturation function and $|X|_a$ is the asymptotic L_∞-norm of the state vector X, then the control system is asymptotically stable.

Proof: The controlled plant with gain γ_1 and restriction Δ_1, and the controller with gain γ_2 and restriction Δ_2 make up of an interconnected system.

1). The interconnected system coincides with Lipschtz well-posed condition.

Since there exists the discontinuous switching control (16), the interconnected system is not globally Lipschtz. But the switching control does not work when the state variables keep sliding on the sliding surfaces and converge to the origin. The interconnected system satisfies the local Lipschtz condition at that time. Thus, we conclude the interconnected system is Lipschtz well-posed.

2). The controller is of asymptotic bound.

Due to the saturation nonlinearity of the controller output, the controller is of asymptotic bound and its gain is less than σ. Its gain function can be defined as

$$\gamma_2(|X|_a) = \min\{|X|_a, \sigma\} \tag{19}$$

3). The controller restriction satisfies $\Delta_2 = \infty$.

The controller input is the output of the controlled plant, namely the state vector X. During the control design, this vector has no constraint. Thus, the controller restriction satisfies $\Delta_2 = \infty$.

4). $\gamma_1(\infty) \le \Delta_1$ is satisfied.

For the interconnected system, we have $\Delta_1 = \sigma$. And the gain function of the controlled plant can be defined as

$$\gamma_1(|u_n|_a) = \min\{|u_n|_a, \sigma\} \tag{20}$$

Thus, there exists $\gamma_1(\infty) \le \sigma = \Delta_1$.

5). From (19) and (20), we have that the composition of the gains γ_1 and γ_2 is a simple contraction.

With the above five conditions, both the controlled plant and the controller are of asymptotic bound by the lemma (nonlinear small gain theorem). Namely, $|X|_a \le \gamma_1(|u_n|_a)$. Hence, let $\sigma > |X|_a$ during the design, then the interconnected system is of asymptotic bound.

If the interconnected system is of asymptotic bound and does not converge to the origin, then the interconnected system is in the reaching mode stage. In this stage, the switching control makes the interconnected system arrive at the sliding mode stage. In the sliding mode stage, the system states keep sliding on the last layer sliding surface and converge to the origin. Moreover, the states of every subsystem keep sliding on the subsystem sliding surface itself and converge to its subsystem origin. Therefore, by combining the conception of the hierarchical sliding mode control, the presented control method can result in an asymptotically stable control system. ■

Remark 1: The conditions $|X|_a < \sigma$ and $\Delta_2 = \infty$ seem contrary. In fact, they do not contradict each other. By considering the interconnected system, the controller input is the state vector X and there is no constraint for X. Furthermore, the inequation $\sigma > |X|_a$ is for control design. It can guarantee the interconnected system is stable. But we don't know the value of $|X|_a$ actually. As a result, we should give a desired value of $|X|_a$ and modify it during simulations.

Theorem 2: Consider the SIMO under-actuated system (1) with the hierarchical sliding mode control law (15) and the ith-subsystem sliding surface (3), assume that all the state variables are equivalent infinitesimals of each other at a certain neighborhood of the origin, then the range of the parameter c_i should be $0 < c_i < |\lim_{X\to 0}(f_i / x_{2i})|$, where X is the state variable vector.

Proof: When the states of the ith subsystem keep sliding on the subsystem sliding surface itself, we have the following equation.

$$\begin{cases} s_i = c_i x_{2i-1} + x_{2i} = 0 \cdots (a) \\ \dot{s}_i = c_i \dot{x}_{2i-1} + \dot{x}_{2i} = 0 \cdots (b) \\ \dot{x}_{2i-1} = x_{2i} \quad \cdots (c) \\ \dot{x}_{2i} = f_i + b_i u_{eqi} \quad \cdots (d) \end{cases} \tag{21}$$

1). Lower boundary of c_i

Replacing x_{2i} in (21a) by (21c), we have

$$s_i = c_i x_{2i-1} + \dot{x}_{2i-1} = 0 \tag{22}$$

Eigenvalue of (22) should be negative for guaranteeing the stability of the ith subsystem. Thus, the lower boundary of c_i is $c_i > 0$.

2). Upper boundary of c_i

Substituting (21d) into (21b), we obtain

$$\dot{s}_i = c_i \dot{x}_{2i-1} + \dot{x}_{2i} = c_i x_{2i} + f_i + b_i u_{eqi} = 0 \tag{23}$$

Further, we have

$$c_i = |(f_i + b_i u_{eqi}) / x_{2i}| \le (|f_i| + |b_i u_{eqi}|) / |x_{2i}| \tag{24}$$

When the states of the ith subsystem keep sliding on its own sliding surface and converge to a certain neighborhood of the origin, this subsystem can be treated as an autonomous system. Thus, we have $c_i \le |f_i / x_{2i}|$.

Further, $c_{i0} = |\lim_{X\to 0}(f_i / x_{2i})|$ can be calculated in light of the assumption in Theorem 2 that all the state variables are equivalent infinitesimals of each other at a certain neighborhood of the origin. As a result, the range of the parameter c_i should be $0 < c_i < c_{i0}$. ■

Remark 2: Although Theorem 2 can not calculate the precise value of c_i, it points out a direction to select the parameter c_i. On the other hand, if a self-adaptive tuning law of c_i is designed, c_i may not be in the open interval $(0, c_{i0})$ when the system states are far from the origin. But c_i will converge to this open interval as the system states converge to the origin.

IV. Simulation Results

The series double inverted pendulum system in Fig. 2 belongs to this class. Its structure contains three subsystems: the upper pendulum, the lower pendulum, and the cart. In this section, we shall demonstrate this control method is applicable to stabilization control of the series double inverted pendulum system. Control objective is to balance both of the pendulums upright and put the cart to the rail origin by moving the cart [9].

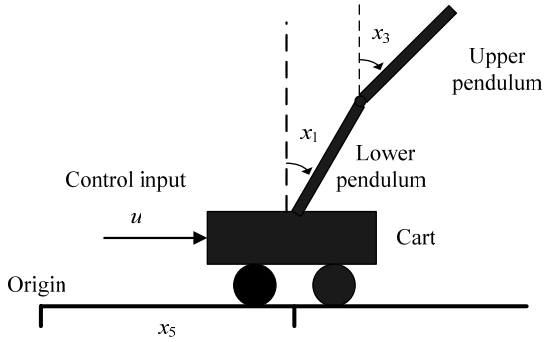

Fig. 2. Structure of the series double inverted pendulum system

The symbols in Fig. 2 are defined as follows: x_1 is the lower pendulum angle with respect to the vertical line; x_3 is the upper pendulum angle with respect to the vertical line; x_5 is the cart position with respect to the origin; u is the control force. Let n=3 in (1). Then we have its state equation, where x_2 is the angular velocity of the lower pendulum; x_4 is the angular velocity of the upper pendulum; x_6 is the velocity of the cart; [10] gave the expressions of f_i and b_i (i=1, 2, 3).

The structural parameters are chosen as the cart mass M=1kg, the lower-pendulum mass m_1=1kg, the upper-pendulum mass m_2=1kg, the lower-pendulum length l_1=0.1m, the upper-pendulum length l_2=0.1m, the gravitational acceleration g=9.81m·s^{-2}, all of which are the same as [9]. The boundaries of c_1, c_2 and c_3 are calculated as 294.39, 98.31 and 11.44, the expressions of which are shown below.

$$\begin{cases} c_{10} = g \left| \dfrac{A^2 (B/3 - m_2 l_2 / 4)}{(m_2/4 - A/3)(B^2 - AC) - m_2 (B - A l_1)^2 / 4} \right| \\ c_{20} = g \left| \dfrac{A^2 (C - B l_1)/2}{l_2 [(m_2/4 - A/3)(B^2 - AC) - m_2 (B - A l_1)^2 / 4]} \right| \\ c_{30} = g \left| \dfrac{AB(B/3 - m_2 l_1 / 4) + A(C m_2 - B m_2 l_1)/2}{(m_2/4 - A/3)(B^2 - AC) - m_2 (B - A l_1)^2 / 4} \right| \end{cases} \tag{25}$$

Here $A = M + m_1 + m_2$, $B = m_1 l_1/2 + m_2 l_1$ and $C = m_1 l_1 l_1/3 + m_2 l_2 l_2$.

The controller parameters are chosen as c_1=184.26, c_2=15.96, c_3=0.72, a_1= -0.06, a_2=0.45, k_3 =37, η_3=0.3 and σ=70 after trial and error. Fig. 3, 4, 5 show the state variables from the initial state vector $X_0 = [\pi/6, 0, \pi/18, 0, 0, 0]^T$ to the desired state vector $X_d = [0, 0, 0, 0, 0, 0]^T$, the entire sliding surfaces, and the control force, respectively. The simulation

results verify the feasibility of the control method.

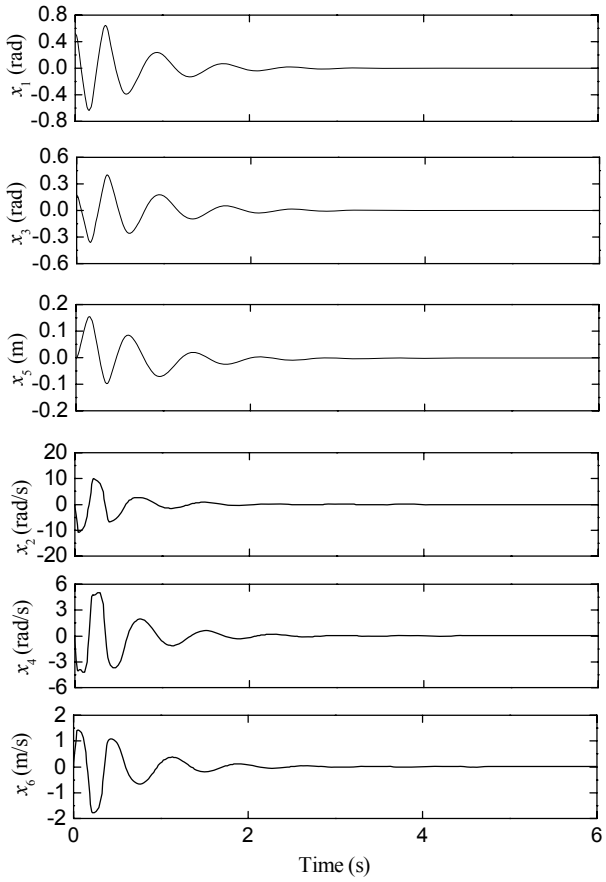

Fig. 3. State variables of the series double inverted pendulum system

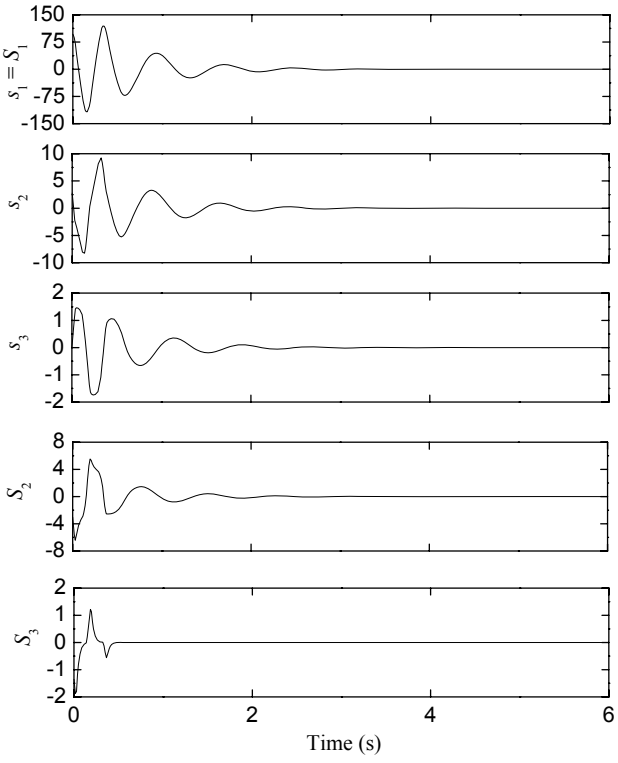

Fig. 4. Subsystem sliding surfaces and Three layer sliding surfaces

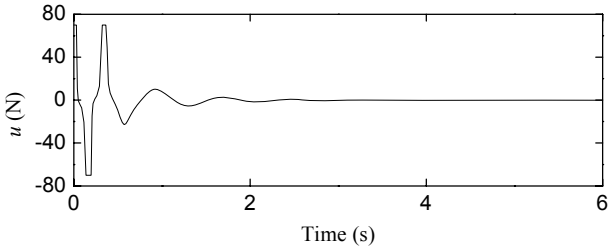

Fig. 5. Control force

Remark 3: Lo's control method [10] could only realize two-level control. Consequently, the controller in [10] could only balance the two pendulums, but failed to put the cart to the origin at the same time. Compared with [10], our control objective is more difficult. The controller parameters in Lin's method [9] were modified by fuzzy logic, but the fuzzy logic made it difficult to analyze system stability. Compared with [9], our curves are smoother and the cart moves shorter under the same physical parameters, the same control objective and the same initial condition.

V. Experimental Results

In this section, the control method is implemented on transport control of an overhead crane testbed system. The 1-dimension crane belongs to this class and is made up of two subsystems: the trolley and the load. Control objective of the transport control is to move the trolley to required position and implement the anti-swing control at the same time. [13] gave the introduction of this testbed in detail.

The physical parameters are determined as the trolley mass M=37.32kg, the load mass m=5.00kg, the rope length l=1.05m, the gravitational acceleration g=9.81m·s^{-2}. Let n=2 in (1). We have its state equation, where x_1 is the trolley position with respect to the origin; x_3 is the swing angle of the load with respect to the vertical line; x_2 is the trolley velocity; x_4 is the angular velocity of the load; u is the single control input; f_i and b_i (i=1, 2) were given in [8].

The controller parameters are chosen as c_1=1.1, c_2=10.3, a_1= -2.9, k_2=1.3, η_2=0.06 and σ=40. c_{10} and c_{20} are calculated as 1.34 and 10.59 from Theorem 2, the expressions of which are shown below.

$$\begin{cases} c_{10} = mg / M \\ c_{20} = (m + M)g /(Ml) \end{cases} \tag{26}$$

Fig. 7 shows all the state variables of the 1-dimension crane system from the initial vector $[0.9,\ 0,\ 0,\ 0]^{\mathrm{T}}$ to the desired vector $[0,\ 0,\ 0,\ 0]^{\mathrm{T}}$. Fig. 8 and Fig. 9 display the curves of the entire sliding surfaces and the single control input added to the trolley, respectively. These results in Figures 7, 8, and 9 coincide with Theorems 1 and 2, which verify the feasibility of the control method.

In Fig. 9, there is one saturating point in the beginning of the simulation transport process, but there are still other saturation points in the experimental transport process besides the beginning. The reason is as follows. The crane

mathematic model was deduced under some assumptions, such as no friction, point mass, etc. But the physical testbed system would not move if there were no friction. These unmodeling and unknown factors make the testbed system need a larger force. Thus, the experimental force curve has more saturation points. The physical experiments show that a small-power actuator could be used to realize the same control objective for a physical system. This case is meaningful for reducing the cost and saving power.

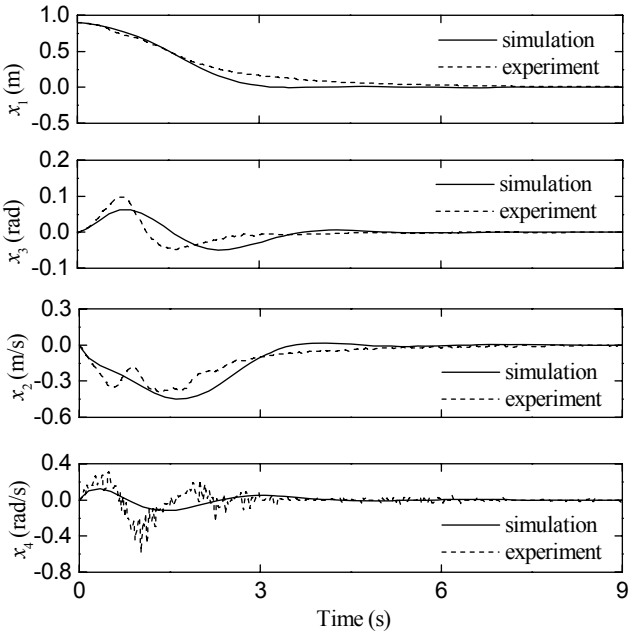

Fig. 7. State variables of the 1-dimension crane system

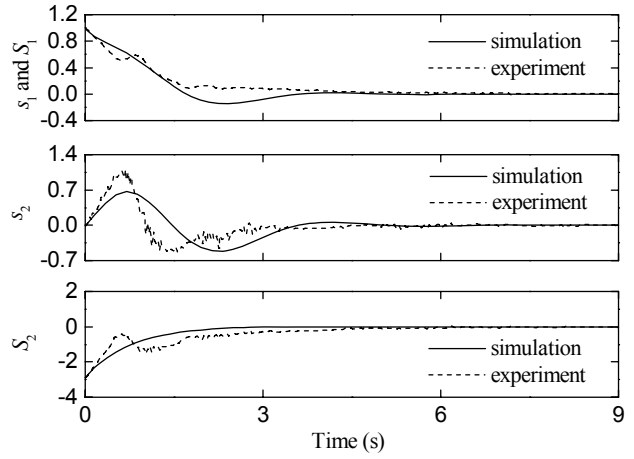

Fig. 8. Entire sliding surfaces

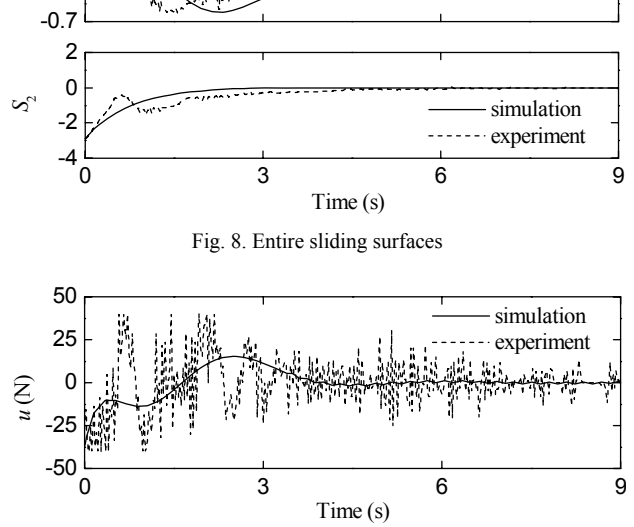

Fig. 9. Control force

VI. Conclusion

The control scheme of a class of SIMO under-actuated systems with saturation using hierarchical sliding mode has been developed. According to the physical structure of the class, the hierarchical sliding surfaces are designed and the hierarchical sliding mode control law is deduced. Due to saturation nonlinearity of the control input, the asymptotic stability of the control system is proven by nonlinear small gain theorem theoretically. The parameter ranges of the subsystem sliding surfaces are also given. In simulation researches, this control method is demonstrated through the stabilization control of a series double inverted pendulum system. In experimental researches, this control method is applied to the transport control of a 1-dimension overhead crane testbed system. The above two under-actuated systems belong to this class with different n, f_i and b_i. Both simulations and experiments confirm the controller's validity and generalization.

References

[1] Ph. Mullhaupt, B. Srinivasan, and D. Bonvin, "Analysis of exclusively kinetic two-link underactuated mechanical systems," *Automatica*, vol.38**,** pp. 1565–1573, Sept. 2002.

[2] I. Fantoni, R. Lozano, and M. W. Spong, "Energy based control of the Pendubot," *IEEE Transactions on Automatic Control*, vol. 45, pp. 725–729, April 2000.

[3] A. Alleyne, "Physical insights on passivity-based TORA control designs," *IEEE Transactions on Control Systems Technology*, vol. 6, pp. 436–439, May 1998.

[4] R. Ortega, M. W. Spong, F. Gomez-Estern, and G. Blankenstein, "Stabilization of a class of underactuated mechanical systems via interconnection and damping assignment," *IEEE Transactions on Automatic Control*, vol. 47, pp. 1218–1233, Aug. 2002.

[5] Y. Fang, W. E. Dixon, D. M. Dawson, and E. Zergeroglu, "Nonlinear coupling control laws for an underactuated overhead crane system," *IEEE/ASME Transactions on Mechatronics*, vol. 8, pp. 418–423, Sept. 2003.

[6] J. Rubi, A. Rubio, and A. Avello, "Swing-up control problem for a self-erecting double inverted pendulum," *IEE Proceedings - Control Theory and Applications*, vol. 149, pp. 169–175, March 2002.

[7] V.I. Utkin, *Sliding modes in control and optimization*. New York: Springer-Verlag, 1992.

[8] W. Wang, J. Yi, D. Zhao, and D. Liu, "Design of a stable sliding- mode controller for a class of second-order under-actuated systems," *IEE Proceedings - Control Theory and Applications*, vol. 151, pp. 683–690, Nov. 2004.

[9] C.M. Lin, and Y.J. Mon, "Decoupling control by hierarchical fuzzy sliding-mode controller," *IEEE Transactions on Control Systems Technology*, vol. 13, pp. 593–598, July 2005.

[10] J.C. Lo, and Y.H. Kuo, "Decoupled fuzzy sliding-mode control," *IEEE Transactions on Fuzzy Systems*, vol. 6, pp. 426–435, Aug. 1998.

[11] W. Wang, X. Liu, and J. Yi, "Structure design of two types of sliding-mode controllers for a class of under-actuated mechanical systems," *IET Control Theory and Applications*, vol. 1**,** pp. 163–172, Jan. 2007.

[12] A.R. Teel, "A nonlinear small gain theorem for the analysis of control systems with saturation," *IEEE Transactions on Automatic Control,* vol. 41, pp. 1256–1270, Sept. 1996.

[13] D. Liu, J. Yi, D. Zhao, and W. Wang, "Adaptive sliding mode fuzzy control for a two-dimensional overhead crane," *Mechatronics*, vol. 15, pp. 505–522, June 2005.